Electronic Supplementary Material (ESI) for Environmental Science: Atmospheres.

Supporting Information: Pros and cons of wood and pellets stoves for residential heating from an emissions perspective

Contents

Iodide FIGAERO Tof-CIMS - sensitivities, sampling, calibration and backgrounds

For the pellet fire sampling, two 2 metre lines of ¼" PFA tubing and copper tubing connected the flue to the ToF-CIMS gas and particle sample lines respectively. A HEPA filter was placed in front of the gas sampling line. Sensitivity was assessed by flowing 30 sccm of N_2 over a vial containing acetic acid (AA) with a critical orifice that restricts emission to 2.0 µg s^{-1} as determined by gravimetric analysis (e.g. Salvador et al., 2019). This flow was diluted by an additional 200 sccm N_2 and periodically sampled every 20 minutes for one minute to assess the instrument sensitivity. Gas phase instrumental backgrounds were performed by flowing 2.5 slm of N_2 to the inlet. This method of backgrounding is considered a good compromise to ensure many compounds have a reasonable, accurate background. Although a compound that is sensitive to water content may exhibit a lower background with dry N_2 as opposed to humidified N_2, the background values are so much lower than the concentrations sampled from the fire that even a large error in background due to water sensitivity would not affect reported concentrations. For example, formic acid, a water sensitive compound, had dry N_2 background concentrations that are 1% of measured concentrations. As the sample flow is diluted with laboratory air, regular sampling of lab air was also performed. The average sensitivity to AA was 3.1 ± 0.6 (1σ) (normalised to 10^6 I^- counts).

The instrument was calibrated using the voltage scanning methodology [2,3]. Briefly, the voltages applied to the SSQ are lowered relative to the BSQ by 12 V in 10 s intervals of 0.5 V to increase the adduct declustering field. The adduct signal decreases as a function of the increasing the declustering field and is described by a sigmoid relationship. The amplitude of this curve (S_0) is shown to exhibit a sigmoidal relationship with dV_{50} (the voltage at which adduct signal is 50% of the maximum theoretical value and is a measure of relative binding energy) and $1/S_0$ describes the maximum theoretical binding of a compound to the reagent ion [2]. A calibration factor for each compound is derived by scaling the experimentally determined calibration factor (Hz ppt^{-1}) for AA by the ratio of the $1/S_0$ for acetic acid (0.7) with the $1/S_0$ for that compound.

$$CF_x = \frac{CF_{AA} \times \frac{1}{S_0{}^x}}{\frac{1}{S_0{}^{AA}}} = \frac{4.0\ Hz\ ppt^{-1}}{0.7} \times \frac{1}{S_0{}^x} \quad (1)$$

Voltage scans were run multiple times during the experiments and an average $1/S_0$ value was used in the calibration factor calculation. The median standard deviation in all derived calibration factors was 30%. A comparison between the voltage scan determined sensitivity and experimentally determined sensitivity for levoglucosan was made to assess the effectiveness of the calibration technique. The voltage scanning derived calibration factor was 1.21 ± 0.18 × 10^4 counts ng^{-1}. The experimental calibration factor was determined by doping a filter with three increasingly larger volumes of a stock levoglucosan in methanol solution and plotting the mass of levoglucosan deposited on the filter against the integrated signal measured with the instrument. This yielded the calibration factor of 1.49 ± 0.15 × 10^4 counts ng^{-1} indicating no significant difference in calibration factor for this compound. Due to time constrains and feasibility of comparing these two methods for every compound, this non-significant difference is assumed for all compounds reported here.

Figaero sampling

For the particle phase, blanks were performed by running a desorption cycle on a filter that was held in an oven overnight at 200°C. Collection on the filter was performed for 5 minutes with a flow of 2 slm N_2. The desorption begins by ramping the temperature of the Figaero to 200°C over 20 minutes and soaking at that temperature for a further 5 minutes. The block was cooled for 5 minutes when collection could then again take place. Data from the cool period is not considered in the analysis.

The maximum temperature of 200°C was not able to capture the full desorption cycle of many lower volatility compounds measured in the particle phase and so defines an innate cut off in the instruments ability to fully quantify very low volatility species. Only particle phase desorptions that exhibit a clear peak are analysed with all others excluded. This has the unfortunate outcome of discounting high mass compounds with Tmaxes greater than the soak temperature of the filter. For the birch fuel, 235 of the 540 thermograms are accepted for analysis and 368 of the 429 are accepted for spruce. Of these 197 and 249 are CHON compounds respectively, of which 149 are common between the two fuel types.

Mono-substituted aromatic compounds (SMAs)

Class	Formula	Mw (g mol^{-1})	potential ID	Reference
	$C_7H_6O_2$	122.0368	Guaiacol	Kong et al., 2021
	$C_8H_8O_2$	136.0524	Phenyl acetate	Kong et al., 2021
	$C_6H_5NO_3$	139.0269	Nitrophenol	Lin et al., 2015
	$C_5H_5NO_4$	143.0219	N/A	Lin et al., 2017
	$C_6H_8O_4$	144.0423	Methylglutaconic acid	Kong et al., 2021
	$C_8H_8O_3$	152.0473	Vanillin	Kong et al., 2021
	$C_7H_7NO_3$	153.0426	Methyl nitrophenol	Mohr et al, 2013
	$C_6H_5NO_4$	155.0219	Nitrocatechol	Lin et al., 2015
	$C_8H_9NO_3$	167.0582	N/A	Lin et al., 2017
SMA	$C_7H_7NO_4$	169.0375	Methyl- nitrocatechol	Lin et al., 2015
	$C_{10}H_{10}O_3$	178.063	N/A	Lin et al., 2017
	$C_{10}H_7NO_3$	189.0426	N/A	Lin et al., 2017
	$C_9H_7NO_4$	193.0375	N/A	Lin et al., 2017
	$C_{10}H_{10}O_4$	194.0579	Acetate vanillin	Kong et al., 2021
	$C_9H_9NO_4$	195.0532	Salicylamide acetic acid	Kong et al., 2021
	$C_{10}H11NO_4$	209.0688	N/A	Fleming et al., 2020
	$C_{10}H_{10}O_5$	210.0528	N/A	Lin et al., 2017
	$C_{10}H_9NO_5$	223.0481	N/A	Lin et al., 2017
	$C_{10}H_{11}NO_5$	225.0637	N/A	Lin et al., 2017

Table S1. List of SMAs identified in this study.

PAHs

Class	Formula	Mw (g mol^{-1})	ID
PAH	$C_{10}H_8$	128.0626	Naphtalene
	$C_{12}H_8$	152.0626	Acenaphthylene
	$C_{12}H_{10}$	154.0782	Acenaphtene
	$C_{13}H_{10}$	166.0782	Fluorene
	$C_{14}H_{10}$	178.0782	Phenantrene
	$C_{14}H_{10}$	178.0782	Anthracene
	$C_{16}H_{10}$	202.0782	Fluoranthene
	$C_{16}H_{10}$	202.0782	Pyrene
	$C_{18}H_{12}$	228.0939	Benzo(a)antrhracene
	$C_{18}H_{12}$	228.0939	Chrysene
	$C_{20}H_{12}$	252.0939	Benzo(b,j)fluoranthene
	$C_{20}H_{12}$	252.0939	Benzo(k)fluoranthene
	$C_{20}H_{12}$	252.0939	Benzo(a)pyrene
	$C_{22}H_{12}$	276.0939	Indeno(123cd)pyrene
	$C_{22}H_{14}$	278.1096	Dibenzo(ah)anthracene
	$C_{22}H_{12}$	276.0939	Benzo(ghi)perylene

Table S2. List of PAHs identified in this study.

Mass loadings

Experiment	OC / µg m^{-3}	BC / µg m^{-3}
Pellet low load	2,496	306
Pellet high load	1,024	154
Birch	1,163	826
Spruce	5,718	2,719

Table S3. Summary of organic aerosol (OC) and black carbon (BC) mass concentrations during Figaero sampling

MCEs

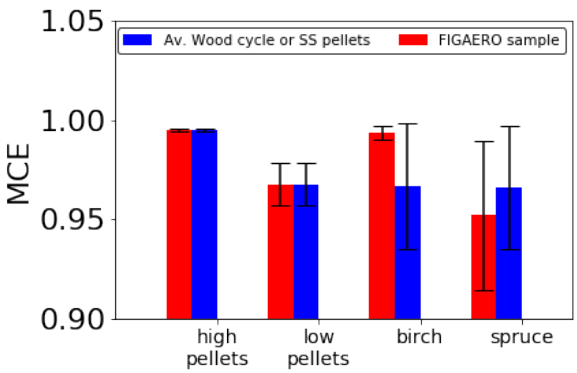

Figure S1. Comparison of modified combustion efficiencies (MCEs) for the 4 different cases during a whole wood cycle or pellet sampling (blue) compared to during the FIGAERO-ToF-CIMS measurement time (red). Note these are the same for the pellet sampling.

Dilution tunnel and dilution

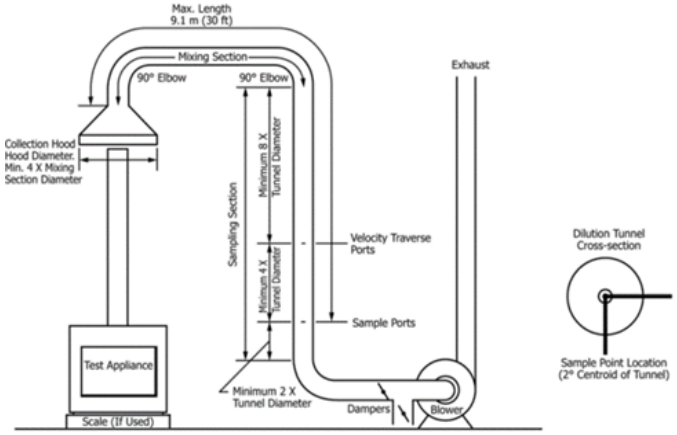

Figure S2. Schematic of the dilution tunnel, Norwegian standard NS3058-1.

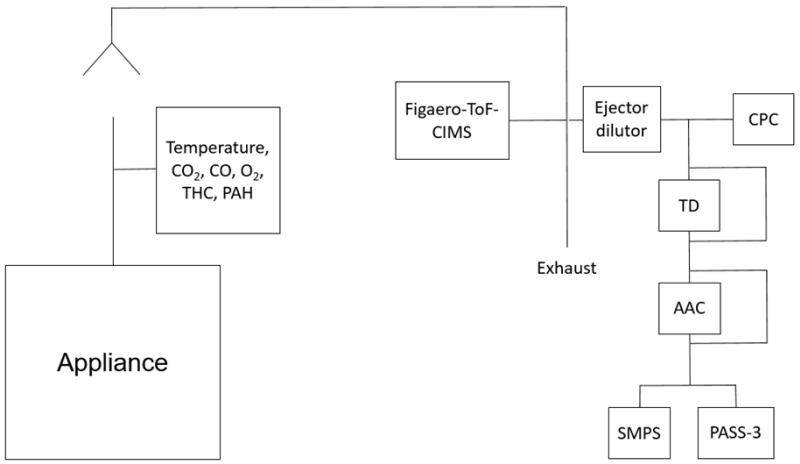

Figure S3. Schematic of measurement setup

Morphological measurements

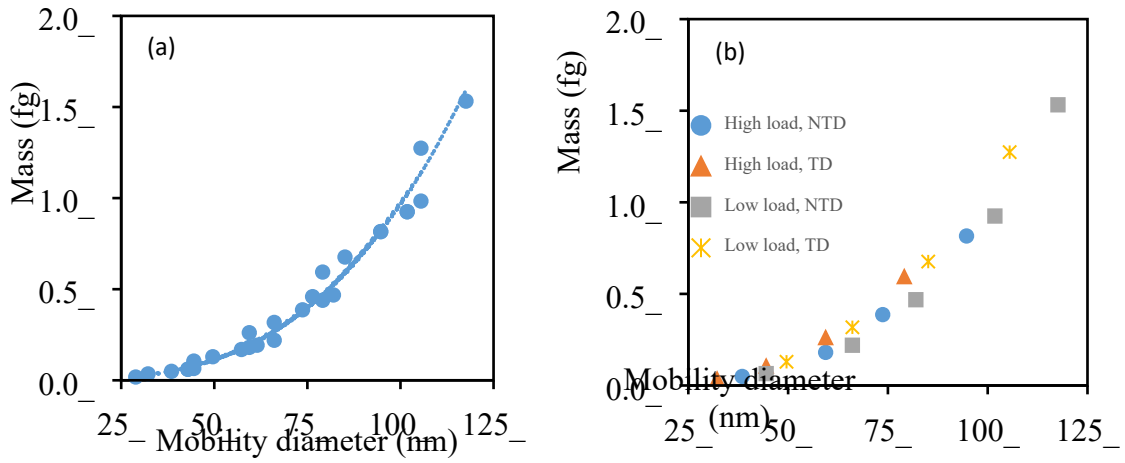

Figure S4. Mass of particles emitted from the pellet stove as a function of mobility diameter. (a) The relationship is cubic indicating the particles are spherical. (b) The relationship is independent of loading or heating (TD: thermal denuder, NTD: No thermal denuder).

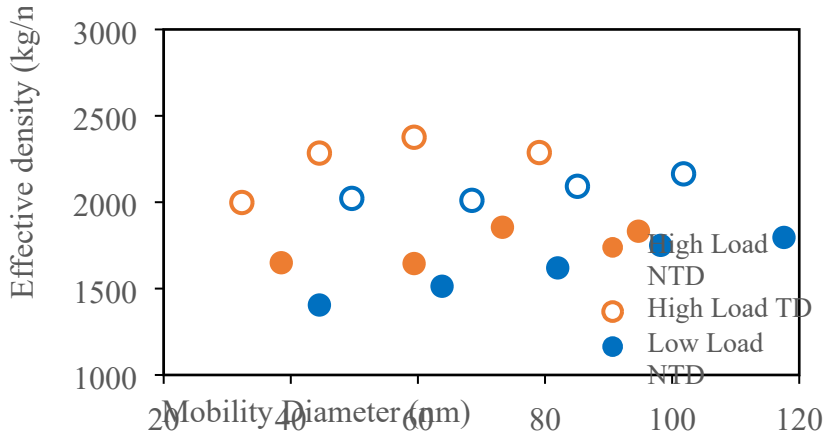

Figure S5. The effective density of the pellet particles as a function of mobility diameter for both loadings, passed through the thermal denuder (TD) and by-passing the TD (NTD). Effective density increases and mobility dimeter decreases when the particles are passed through the TD suggesting a loss of semi-volatile organic material thus relatively increasing the proportion of measured mass due to non-refractory material e.g. a black carbon core.

References

1 C. M. Salvador, G. Bekö, C. J. Weschler, G. Morrison, M. Le Breton, M. Hallquist, L. Ekberg and S. Langer, *Indoor Air*, 2019, **29**, 913–925.

2 F. D. Lopez-Hilfiker, S. Iyer, C. Mohr, B. H. Lee, E. L. D'Ambro, T. Kurtén and J. A. Thornton, *Atmos. Meas. Tech. Discuss.*, 2015, **8**, 10875–10896.

3 D. J. Price, D. A. Day, D. Pagonis, H. Stark, L. B. Algrim, A. V. Handschy, S. Liu, J. E. Krechmer, S. L. Miller, J. F. Hunter, J. A. de Gouw, P. J. Ziemann and J. L. Jimenez, *Environ. Sci. Technol.*, 2019, **53**, 13053–13063.